Received: 22 January 2019 | Revised: 10 April 2019 | Accepted: 11 April 2019

DOI: 10.1002/jcp.28751

ORIGINAL RESEARCH ARTICLE

WILEY Journal of Cellular Physiology

Genome-wide microRNA screening reveals miR-582-5p as a mesenchymal stem cell-specific microRNA in subchondral bone of the human knee joint

Pinger Wang[1,2,3*] | Rui Dong[1,2,3*] | Baoli Wang[4] | Zhaohuan Lou[5] | Jun Ying[1] | Chenjie Xia[1] | Songfeng Hu[6] | Weidong Wang[7] | Qi Sun[8] | Peng Zhang[1] | Qinwen Ge[1] | Luwei Xiao[3] | Di Chen[9] | Peijian Tong[1,2] | Ju Li[1,2] | Hongting Jin[1,2,3]

[1]The First Clinical Medical College, Zhejiang Chinese Medical University, Hangzhou, Zhejiang, China

[2]Department of Orthopaedic Surgery, The First Affiliated Hospital of Zhejiang Chinese Medical University, Hangzhou, Zhejiang, China

[3]Institute of Orthopaedic and Traumatology of Zhejiang Province, Hangzhou, Zhejiang, China

[4]Key Laboratory of Hormones and Development, Ministry of Health, Tianjin Metabolic Diseases Hospital, Tianjin Institute of Endocrinology, Tianjin Medical University, Tianjin, China

[5]The Pharmaceutical College, Zhejiang Chinese Medical University, Hangzhou, Zhejiang, China

[6]Department of Orthopaedics, Shaoxing Hospital of Traditional Chinese Medicine, Shaoxing, Zhejiang, China

[7]Department of Orthopaedic Surgery, The Second Affiliated Hospital of Zhejiang Chinese Medical University, Hangzhou, Zhejiang, China

[8]Department of Orthopaedic Surgery, Fuyang Orthopaedics and Traumatology Affiliated Hospital of Zhejiang Chinese Medical University, Hangzhou, Zhejiang, China

[9]Department of Orthopedic Surgery, Rush University Medical Center, Chicago, Illinois

Correspondence
Hongting Jin, Department of Orthopaedic Surgery, The First Affiliated Hospital of Zhejiang Chinese Medical University, Youdian Road, No. 54, Shangcheng District, Hangzhou, 310006 Zhejiang, China.
Email: hongtingjin@163.com
Ju Li, Department of Orthopaedic Surgery, The First Affiliated Hospital of Zhejiang Chinese Medical University, Youdian Road, No. 54, Shangcheng District, Hangzhou, 310006 Zhejiang, China.
Email: 48490441@qq.com
Peijian Tong, Department of Orthopaedic Surgery, The First Affiliated Hospital of Zhejiang Chinese Medical University, Youdian Road, No. 54, Shangcheng District, Hangzhou, 310006 Zhejiang, China.
Email: peijiantongzjtcm@163.com

Funding information
National Natural Science Foundation of China, Grant/Award Numbers: 81873325, 81774346, 81774332, 81873324; Zhejiang grants funded by Provincial Natural Science Foundation of China, Grant/Award Numbers: LY18H270004, LY16H270010; Project of

Abstract

Emerging evidence suggests that microRNAs (miRNAs) may be pathologically involved in osteoarthritis (OA). Subchondral bone (SCB) sclerosis is accounted for the knee osteoarthritis (KOA) development and progression. In this study, we aimed to screen the miRNA biomarkers of KOA and investigated whether these miRNAs regulate the differentiation potential of mesenchymal stem cells (MSCs) and thus contributing to SCB. We identified 48 miRNAs in the blood samples in KOA patients ($n = 5$) through microarray expression profiling detection. After validation with larger sample number, we confirmed hsa-miR-582-5p and hsa-miR-424-5p were associated with the pathology of SCB sclerosis. Target genes prediction and pathway analysis were implemented with online databases, indicating these two candidate miRNAs were closely related to the pathways of pluripotency of stem cells and pathology of OA. Surprisingly, mmu-miR-582-5p (homology of hsa-miR-582-5p) was downregulated in osteogenic differentiation and upregulated in adipogenic differentiation of mesenchymal progenitor C3H10T1/2 cells, whereas mmu-mir-322-5p (homology of hsa-miR-424-5p) showed no change through the in vitro study. Supplementing mmu-miR-582-5p mimics blocked osteogenic and induced adipogenic differentiation of C3H10T1/2 cells, whereas silencing of the endogenous mmu-miR-582-5p enhanced

*Pinger Wang and Rui Dong contributed equally to this work.

Zhejiang Chinese Medical University, Grant/Award Number: 2C01801–01; State Administration of Traditional Chinese Medicine of Zhejiang Province, Grant/Award Numbers: 2018ZA034, 2018ZZ011, 2019ZQ018

osteogenic and repressed adipogenic differentiation. Further mechanism studies showed that mmu-miR-582-5p was directly targeted to Runx2. Mutation of putative mmu-miR-582-5p binding sites in Runx2 3′ untranslated region (3′UTR) could abolish the response of the 3′UTR-luciferase construct to mmu-miR-582-5p supplementation. Generally speaking, our data suggest that miR-582-5p is an important biomarker of KOA and is able to regulate osteogenic and adipogenic differentiation of MSCs via targeting Runx2. The study also suggests that miR-582-5p may play a crucial role in SCB sclerosis of human KOA.

KEYWORDS

knee osteoarthritis, mesenchymal stem cells, miR-582-5p, subchondral bone

1 | INTRODUCTION

Knee osteoarthritis (KOA) is the most common degenerative joint disease and affects >1.12 billion residents in China (Tang et al., 2016). Clinically, the KOA victims present as radiographic narrowing of joint space accompanied with articular cartilage destruction, subchondral bone (SCB) sclerosis and osteophyte formation at joint margin, resulting in chronic joint pain and physical disability (Lawrence,et al., 2008). Current treatment strategies could not effectively delay or attenuate the progression of the disease. Although great efforts were taken into the research of KOA, no one can explain the exact pathogenesis of the disease.

Understanding the underlying pathogenesis and mechanisms could facilitate the development of novel therapies. Articular cartilage degradation is the primary concern in KOA (Zhen et al., 2013) as it usually appears earlier (Juneja, Ventura, Jay, & Veillette, 2016), but the importance of other joint tissues especially SCB cannot be ignored. A growing number of investigators preferred to define KOA as a disease of the whole joint, the integrity and hemostasis of articular cartilage rely on the biochemical and biomechanical interplay with SCB and other joint tissues (Lories & Luyten, 2011). At the early stage of KOA, the articular cartilage and SCB interface underwent remodeling, especial beneath the regions of articular cartilage damage which eventually cause SCB sclerosis and finally precede cartilage degeneration in return. Several reports suggest that SCB changes involved in the onset of KOA. SCB provides mechanical support for the overlying articular cartilage and bears most of the mechanical force. Furthermore, it also counts for the metabolism of articular cartilage (Madry, van Dijk, & Mueller-Gerbl, 2010). A recent study showed that inhibition of SCB sclerosis could attenuate osteoarthritis (OA) progression (Zhen et al., 2013). Apparently, effective prevention of SCB sclerosis might be a key objective of new therapeutic approaches.

In consideration of the effectiveness of current treatment, the major challenge faced by KOA research is early diagnosis and identify patients with fast progression of KOA disease (Glyn-Jones, Palmer, & Agricola, 2015). Clinically, KOA is diagnosed radiographically when clinical signs of pain and stiffness have already appeared. Moreover, many patients were diagnosed in the middle and late stages. Therapeutic intervention in OA has been limited by insufficient approaches of early diagnosis (Kung et al., 2017). Above all, it is urgently needed to developing sensitive and specific biomarkers not only for early diagnosis but also for the novel strategy for clinical treatment.

MicroRNAs (miRNAs) are short noncoding 18–24 nucleotides RNAs that regulate target genes expression by influencing messenger RNA (mRNA) degradation and/or inhibiting RNA expression, and they have been found in different organisms. Previous data showed that about 30% mammalian mRNAs seem to be regulated by miRNAs (Lewis, Burge, & Bartel, 2005). Recently, increasing evidence indicated miRNAs as promising diagnostic biomarkers for many diseases including gastric cancer (Kao et al., 2017), renal cell carcinoma (Petrozza et al., 2017) and atherogenesis (Vilahur, 2017). Furthermore, miRNAs also acted as potential targets for therapeutic. In KOA, miRNAs cannot only predict early cartilage degeneration (Kung et al., 2017), but also have the function of proinflammation and catabolism/anabolism in the pathophysiology of the disease (Alcaraz, Megías, García-Arnandis, Clérigues, & Guillén, 2010). It has been reported that regulation of miRNAs expression could prevent matrix degradation and cartilage degeneration (Chen & Tian, 2017; Yu & Wang, 2018). Although several studies are exploring the role of miRNA in KOA, they tend to focus on cartilage degradation, but not the role of miRNAs in SCB.

As SCB plays an important role in KOA development, we hypothesized that circulating miRNAs may have a significant role in KOA subchondral bone sclerosis. To confirm this hypothesis, we have performed following studies: (a) measuring the expression differences of circulating miRNA between KOA patients and non-KOA subjects; (b) validating the data using larger sample size; (c) validating the candidate miRNAs using an independent set of SCB specimens; (d) analyzing data using Gene Ontology (GO) analysis and Kyoto Encyclopedia Genes and Genomes (KEGG) pathway analysis to identify the target genes and signaling pathways; (e) investigating the exact role of candidate miRNA by transfection in mesenchymal stem cells (MSCs).

2 | MATERIALS AND METHODS

2.1 | Patients and human samples

Whole blood samples were collected from the KOA patients (diagnosed according to the criteria listed in Figure 1b, $n = 31$) and age-matched non-KOA volunteers ($n = 22$) at the first affiliated hospital of Zhejiang Chinese Medical University. At least 3 ml peripheral blood was mixed with 9 ml red blood cells lysis buffer, the supernatant was removed after a brief centrifugation and stored at −80°C until further use. We screened five KOA and five non-KOA blood samples, respectively, for further miRNA microarray expression profiling to detect differentially expressed circulating miRNAs (Figure 1a). SCB was obtained from the KOA individuals intraoperatively, severe KOA sclerotic bone (showed complete cartilage degeneration with exposed bone, $n = 6$) and nonsclerotic KOA bone (showed full cartilage thickness on top of it, $n = 4$) were separated from the specimens as previously reported (Prasadam et al., 2016), immediately scanned for micro-CT analysis and stored at −80°C for miRNAs detection. All methods were performed in accordance with the relevant guidelines and regulations of Zhejiang Chinese Medical University and were approved by its ethical committee.

2.2 | RNA and miRNA extraction

Total RNA was extracted from blood and SCB using mirVana™ RNA Isolation Kit (Thermo Fisher Scientific, MA, p/n AM1556) according to the manufacturer's instructions. The yield of RNA was measured by NanoDrop spectrophotometer (Thermo Fisher Scientific), and the integrity was evaluated using agarose gel electrophoresis stained with ethidium bromide.

2.3 | miRNA expression profiling

Global miRNA expression profiling was conducted using microarray manufactured by Agilent Technologies (Agilent Technologies Inc, CA). Labeling and hybridization of total RNA samples were performed with miRNA complete Labeling and Hyb Kit (Agilent Technologies Inc, p/n 5190-0456) according to the manufacturer's protocol. PCp-Cy3 labeled miRNA samples were hybridized for at least 20 hr at 55°C on Agilent Human miRNA chips (Agilent human miRNA Microarray miRBase Release 19.0, 8×60K, Design ID: G4872A-046064). The hybridization signals were analyzed through a G2505C Agilent Scanner and specialties were extracted using Agilent Feature Extraction 12.0.07 software. The signal after background subtraction was exported directly into the GeneSpring software (version 12.5, Agilent Technologies Inc) that were used to normalization for further use. The fold changes of the circulating miRNA expression between samples of healthy controls and OA patients were calculated from the signal values. miRNA expression was considered significantly different if the fold change >2.

2.4 | Validation of candidate mature miRNAs by quantitative real-time polymerase chain reaction (qRT-PCR)

qRT-PCR was performed using LightCycler® 480 II Real-time PCR Instrument (Roche, Basel, Swiss) to analysis the quantification of candidate mature miRNAs in human samples. Each sample was analyzed in triplicate. The primer sequences of miRNAs were designed and synthesized by Generay Biotech (Generay, Shanghai, China) according to the miRBase database (Release 20.0) in Table 1. The expression levels of miRNAs were normalized to U6 respectively as endogenous control and were calculated using the $2^{-\Delta\Delta C_t}$ method (Livak & Schmittgen, 2001).

(a)

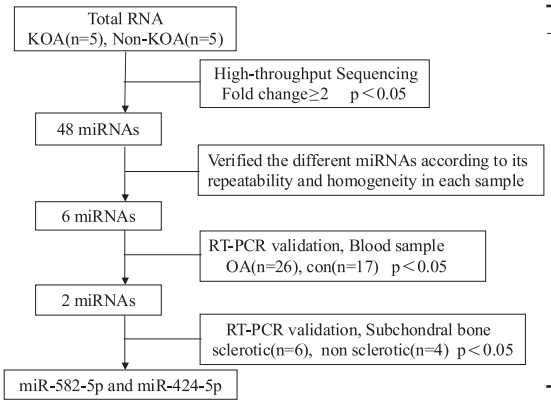

(b)

Group	Criteria
KOA individuals	**Inclusion criteria:**
	Age between 55 and 65 years
	Diagnosed on the basis of American college of Rheumatology criteria for knee OA[15].
	The Kellgren-Lawrence score ≥2
	Exclusion criteria:
	Presenting other disease which might affected bone metabolism
	Presenting an additional rheumatologic involvement, such as systemic disease, spondylitis and rheumatoid arthritis.
	Presenting history of serious knee injuries
Non-KOA group	Age-related person without KOA and any other arthritis diseases which undertaken treatment for injuries (bone fractures, contusions, etc.)

FIGURE 1 (a) A flowchart illustrates how we identified circulating miRNAs. We performed a systematic miRNA analysis on blood samples from KOA patients ($n = 5$) and healthy controls ($n = 5$), 48 circulating miRNAs have significant ($p < 0.05$) changes in expression. Six candidate miRNAs have been selected after we verified the different miRNAs according to their repeatability and homogeneity in each sample. Two different expressed miRNAs were confirmed with blood from 26 OA patients and 17 health control using real-time polymerase chain reaction assay. These two miRNAs were measured in severe KOA sclerotic SCB ($n = 6$) and nonsclerotic SCB ($n = 4$) to confirm the expression difference. (b) Inclusion and exclusion criteria of the patients recruited for this study. KOA: knee osteoarthritis; miRNA: microRNA; OA: osteoarthritis; SCB: subchondral bone

TABLE 1 Primers used for the quantitative real-time polymerase chain reaction

Name	Primer sequence
hsa-miR-371a-5p	5′-ACTCAAACTGTGGGGGCACT-3′
hsa-miR-197-3p	5′-TTCACCACCTTCTCCACCCAGC-3′
hsa-miR-125a-3p	5′-ACAGGTGAGGTTCTTGGGAGCC-3′
hsa-miR-582-5p	5′-TTACAGTTGTTCAACCAGTTACT-3′
hsa-miR-338-3p	5′-TCCAGCATCAGTGATTTTGTTG-3′
hsa-miR-424-5p	5′-CAGCAGCAATTCATGTTTTGAA-3′
mmu-miR-322-5p	5′-CAGCAGCAATTCATGTTTTGGA-3′
mmu-miR-582-5p	5′-ATACAGTTGTTCAACCAGTTAC-3′
mmu-U6	5′-TTCGTGAAGCGTTCCATATT-3′
PPARγ forward	CTTGACAGGAAAGACAACGG
PPARγ reverse	GCTTCTACGGATCGAAACTG
C/EPBα forward	CTGATTCTTGCCAAACTGAG
C/EPBα reverse	GAGGAAGCTAAGACCCACTAC
Runx2 forward	TCCTGTAGATCCGAGCACCA
Runx2 reverse	CTGCTGCTGTTGTTGCTGTT
ALP forward	GTTGGGGGTGCCCACGGT
ALP reverse	CCTTGGACAGAGCCATGTATG
β-Actin forward	GGAGATTACTGCCCTGGCTCCTA
β-Actin reverse	GACTCATCGTACTCCTGCTTGCTG

Note. hsa-miR-424-5p and hsa-miR-582-5p are highly homologous to mmu-miR-322-5p and mmu-miR-582-5p, respectively, as showed in miRbase (www.mirbase.org).
ALP: alkaline phosphatase; PPARγ: peroxisome proliferator-activated receptor γ.

2.5 | Prediction of genes/pathways regulated by miRNAs

Targetscan, MicroRNA, and PITA were used to predict candidate miRNAs targets. An mRNA that considered as a potential target only if it appeared in all three databases. GO and KEGG pathway analyses were used to identify relevant miRNAs biological pathways.

2.6 | Micro-computed tomography (μCT) analysis

The SCB samples harvested from KOA individuals intraoperatively described above were placed into a 16 mm tube filled with phosphate-buffered saline (RNase free) and scanned by Skyscan1176 μCT scanner (Bruker, Kontich, Belgium) with a scan resolution of 35 μm. Images were used for three-dimensional (3D) reconstruction of bone microstructure and quantitative analysis of bone parameters.

2.7 | Cell culture and osteogenic/adipogenic differentiation assay

C3H10T1/2 Mesenchymal progenitor cells were provided by professor Baoli Wang (Tianjin Medical University) and cultured in Dulbecco's modified Eagle's medium (DMEM, HyClone, UT, p/n: SH30243.01) which contained 10% fetal bovine serum (FBS) plus 50 U/ml penicillin and 50 mg/ml streptomycin. The expend-cultured cells then were cultured in the osteoblast-induced medium (OIM, DMEM supplemented with 10% FBS, 50 μg/ml of ascorbic acid and 10 mM β-glycerophosphate) to induce osteogenic differentiation. To induce adipogenic differentiation, cells were induced in the adipocyte-inducing medium (AIM, DMEM supplemented with 10% FBS, 1 M dexamethasone, 0.5 mM methylisobutylxanthine, 10 g/ml of insulin, and 100 M indomethacin) for 3 days and then cultured in the following adipocyte-maintaining medium (AMM, DMEM supplemented with 10% FBS and 10 μg/ml of insulin) for 2 days.

2.8 | Validation of candidate miRNAs in differentiated cells

Previously selected candidate miRNAs were testified in two differentiated cells: Osteogenic differentiation cells and adipogenic differentiation cells. mmu-miR-582-5p and mmu-miR-322-5p were highly homologous with hsa-miR-582-5p and hsa-miR-424-5p as showed in MiRbase (www.mirbase.org), respectively. After differentiation, two differentially expressed miRNAs were validated in these cells by qRT-PCR.

2.9 | Transfection

The synthetic mimics or inhibitors of mmu-miR-582-5p (GenePharma, Shanghai, China) were transfected into C3H10T1/2 cultures by using Lipofectamine™ RNAiMAX Transfection Reagent (Invitrogen, Carlsbad, CA) according to the manufacturer's procedure before differentiation. Transfection efficiency was measured by percentage of the fluorescent-positive cell through fluorescence microscope 16 hr after transfection. Cells were induced for different periods of time and then harvested.

2.10 | Luciferase reporter assay

Target mRNAs were predicted as described above. The 3′ untranslated region (3′UTR) fragments carrying the putative or mutant miRNA binding sites were PCR-amplified using mouse complementary DNA (cDNA) as the template. The primers used for amplification were: Low-density lipoprotein receptor-related protein 6 (LRP6), LRP6 sense: 5′-GCGCAC TAGTGAGGGAGCTCATGGTGCTTTGCAAGGATGTA-3′, LRP6 antisense: 5′-AAAGATCCTTTATTAAGCTTTCCACTGATTTTTCCACTGT-3′; Rapamycin-insensitive companion of mammalian target of rapamycin (RICTOR), RICTOR sense: 5′-GCGCACTAGTGAGGGAGCTCATACGCTG CTACATTTTTGGAGG-3′, RICTOR antisense: 5′-AAAGATCCTTTATTA AGCTTAGTGAGCAAAACCATTTTGGGAC-3′; Runt-related transcription factor 2 (Runx2), WT-Runx2 sense: 5′-CTGAACTTCAAAGGGACTAT TTGTATTGT ATGTTGCAACTGTAAATTGAATTATTTGGCATTTCC-3′, WT-Runx2 antisense: 5′-TCGAGGA AATGCCAAATAATTCAATTTACAG TTGCAACATACAATACAAATAGTCCCTTTGAAGTTCAGAGCT-3′, mut-Runx2 sense: 5′-CTGAACTTCAAAGGGACTATTTGTATTGTATCAACGT

TG ACATAATTGAATTATTTGGCATTTCC-3′, mut-Runx2 antisense: 5′-TCGAGGAAATGCCAAAT AATTCAATTATGTCAACGTTGATACAATACAAATAGTCCCTTTGAAGTTCAGAGCT-3′. The PCR products were cloned into pMir-report vector (for LRP6 and RICTOR) at *Sac*I/*Hin*dIII sites, or into pmirGLO vector (for Runx2) at *Sac*I/*Xho*I sites using the ClonExpress II One Step Cloning Kit (Vazyme, Nanjing, China). miR-mimics or its negative control was cotransfected into HEK-293 cells along with the 3′ UTR constructs in a 24-well plates. The Renilla luciferase reporter plasmid pRL-SV40 was also included for the cotransfection to monitor the transfection efficiency (for pMir-report vector). The cells were harvested 36 hr after transfection and luciferase activity was measured using a dual-luciferase reporter assay kit (Promega, San Luis Obispo, CA). The relative firefly luciferase activity was determined as the ratio of firefly to Renilla luciferase activity.

2.11 | Alkaline phosphatase (ALP)/oil red O staining

After 16 hr transfection, the cells were cultured in 24-well plates for osteogenic/adipogenic induction. ALP staining was conducted by 1-Step™ NBT/BCIP Kit (Thermo Fisher Scientific, p/n: 34042) according to the manufacturer's procedure after osteogenic induced for 9 days. Oil red O staining was conducted by Oil red O Staining Kit (ScienCell, p/n:0843) according to the manufacturer's procedure after adipogenic induced for 5 days as previously described.

2.12 | qRT-PCR and western blot analysis for osteogenic/adipogenic differentiation markers

After 16 hr transfection, the cells were cultured in six-well plates for osteogenic/adipogenic differentiation induction. For qRT-PCR, the cells were induced in OIM/AIM for 2 days. Total RNA was obtained by TRIzol® Reagent (Invitrogen, p/n:15596-026), cDNA was synthesized using PrimeScript™ RT Reagent Kit (Takara, Beijing, China, p/n: rr037A) following the manufacturer's procedure. qRT-PCR was conducted by SYBR® Premix Ex Taq™ II (Takara, p/n: rr820A). Expression levels of several genes were normalized by β-actin. For western blot assay, the cells were induced in OIM/AIM for 3 days and lysed on ice for 30 min in a radioimmunoprecipitation assay (RIPA) lysis buffer (CW Biotech, Beijing, China, p/n: cw2334) contain ethylenediaminetetraacetic acid (EDTA)-free Protease Inhibitor Cocktail (Roche, p/n:04693132001). Proteins were quantified through Pierce™ BCA Protein Assay Kit (Thermo Fisher Scientific, p/n:23225) and fractionated by sodium dodecyl sulfate polyacrylamide gel electrophoresis, transferred to a nitrocellulose membrane. After blocking at room temperature for 2 hr in the solution that contains 5% of fat-free milk, the membranes were incubated overnight at 4°C with primary antibodies. After several washes, the fluorescent secondary antibody was used to incubate the membranes at room temperature without lighting for 2 hr. The expression of these proteins was then detected by Odyssey® CLX Imaging System (LI-COR Biosciences, NE) according to the manufacturer's recommendation. The primary antibodies were as follow: rabbit anti-rat anti-RUNX2 antibody (1:1,000, 8486; Cell Signaling Technology, Boston), rabbit anti-rat anti-ALP antibody (1:1,000, ARG57422; Arigo, Taiwan, China), rabbit anti-rat anti C/EBPα antibody (1:1,000, 8178S; Cell Signaling Technology), rabbit anti-rat anti-PPARγ (peroxisome proliferator-activated receptor γ) antibody (1:1,000, ARG55241; Arigo), and mouse anti-rat anti-β-actin antibody (1:10,000, A1978; Sigma-Aldrich, St. Louis). The second antibodies were as follow: IRDye 800CW Goat anti-rabbit IgG (H + L) (1:10,000, 926-32211; Biocompare, South San Francisco) and IRDye 680RD Goat anti-mouse IgG (H + L) (1:10,000, 926-68070; Biocompare).

2.13 | Statistical analysis

In the present work, the statistical package for the social sciences (version 24.0; SPSS Inc, Chicago, IL) was used to perform statistical analysis. The results were presented as mean and standard deviation. An independent the Student *t* test was used to examine statistical comparison. $p < 0.05$ considered as statistically significant variation between groups.

3 | RESULTS

3.1 | hsa-miR-582-5p and hsa-miR-424-5p were downregulated in KOA blood compared with non-KOA

First, we performed global miRNA profiling in blood from five KOA patients and five healthy controls to figure out the difference between two groups. Briefly, we used Agilent Human miRNA chips that contain 60,000 probes for 1,888 human microRNAs (miRbase 19.0). After probe screening and data normalization, we found 48 significantly and differentially expressed miRNAs between two groups, which contains 39 upregulated miRNAs and 9 downregulated miRNAs (Figure 2a,b). We next verified the expression tendency for candidate miRNAs in these 10 samples by qRT-PCR. Surprisingly, 42 candidate miRNAs were not showed the same expression tendency in the samples of the same group, whereas six candidate miRNAs include two upregulated miRNAs and four downregulated miRNAs were confirmed to the next validation stage as follow: hsa-miR-424-5p, hsa-miR-371a-5p, hsa-miR-197-3p, hsa-miR-125a-3p, hsa-miR-582-5p, and hsa-miR-338-3p. We then enlarged the blood samples of KOA patients ($n = 26$) and non-KOA controls ($n = 17$) to further confirm the six candidate miRNAs expression in two groups. As a result, hsa-miR-582-5p and hsa-miR-424-5p were significantly decreased in KOA patients, conversely, another four miRNAs showed no difference between two groups (Figure 2c).

(a)

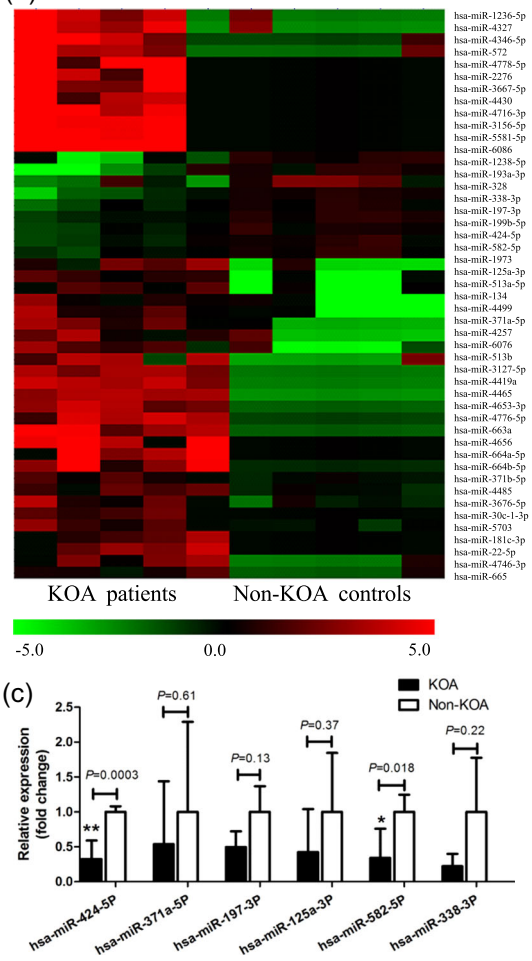

(b)

Number	systematic_name	P value	FC (abs)	Regulation
1	hsa-miR-1227-3p	0.023033459	6.4051385	down
2	hsa-miR-1236-5p	0.0375994	15.96241	up
3	hsa-miR-1238-5p	0.023319343	6.100742	down
4	hsa-miR-125a-3p	0.013660129	18.574709	up
5	hsa-miR-134	0.026599007	20.48074	up
6	hsa-miR-181c-3p	0.039570555	2.7091324	up
7	hsa-miR-193a-3p	0.027752679	9.286151	down
8	hsa-miR-197-3p	0.001779956	2.216446	down
9	hsa-miR-1973	0.00428833	23.271612	up
10	hsa-miR-199b-5p	0.016423097	2.060923	down
11	hsa-miR-22-5p	0.012265377	4.5892925	up
12	hsa-miR-2276	0.020816114	10.604551	up
13	hsa-miR-30c-1-3p	0.01388434	2.3548057	up
14	hsa-miR-3127-5p	8.07E-08	34.129707	up
15	hsa-miR-3156-5p	0.005541537	21.914423	up
16	hsa-miR-328	0.008572564	4.4879003	down
17	hsa-miR-338-3p	0.027532833	2.297094	down
18	hsa-miR-3667-5p	0.029447304	12.138587	up
19	hsa-miR-3676-5p	0.0445858	3.8108816	up
20	hsa-miR-371a-5p	0.001400742	19.687626	up
21	hsa-miR-371b-5p	0.03574692	2.0051243	up
22	hsa-miR-424-5p	0.014037964	2.1605916	down
23	hsa-miR-4257	0.01833241	13.610614	up
24	hsa-miR-4327	0.03826586	20.418037	up
25	hsa-miR-4419a	4.38E-08	54.255745	up
26	hsa-miR-4430	0.024801917	8.111456	up
27	hsa-miR-4465	2.18E-10	61.25763	up
28	hsa-miR-4485	0.006592447	2.9941018	up
29	hsa-miR-4499	0.015120752	29.748005	up
30	hsa-miR-4646-5p	0.020323085	13.606736	up
31	hsa-miR-4653-3p	3.71E-06	25.461494	up
32	hsa-miR-4656	0.006294024	14.303293	up
33	hsa-miR-4716-3p	0.008090745	16.997326	up
34	hsa-miR-4746-3p	0.005588433	9.959537	up
35	hsa-miR-4776-5p	4.20E-05	22.131136	up
36	hsa-miR-4778-5p	0.028158836	35.790096	up
37	hsa-miR-513a-5p	0.021829609	21.474306	up
38	hsa-miR-513b	0.021128237	16.469498	up
39	hsa-miR-5581-5p	0.004806061	20.29832	up
40	hsa-miR-5703	0.024462061	2.8856485	up
41	hsa-miR-572	0.035799578	12.1692295	up
42	hsa-miR-582-5p	0.01647421	2.015411	down
43	hsa-miR-6076	0.018536469	17.274977	up
44	hsa-miR-6086	0.004725969	34.602856	up
45	hsa-miR-663a	3.20E-05	42.177963	up
46	hsa-miR-664a-5p	0.012146443	10.071006	up
47	hsa-miR-664b-5p	0.002075268	16.962912	up
48	hsa-miR-665	0.011640349	3.6162512	up

(c)

FIGURE 2 Expression of hsa-miR-582-5p and hsa-miR-424-5p was reduced in the blood samples from patients with KOA. (a) Heat map summarizing expression values of 48 miRNAs KOA and in non-KOA patients. Color range from green (low expression) to red (high expression). (b) The list of 48 differential expression miRNAs, highlighted miRNAs were selected to the validation stage as they showed the same expression tendency in each sample of the same group. (c) Enlarged sample validation indicates that expression of hsa-miR582-5p and hsa-miR424-5p was significantly downregulated in KOA patients' samples, the other four miRNAs show no difference between two groups. All data are shown as mean ± SD. $^{*}p < 0.05$, $^{**}p < 0.01$. p Values were determined by the Student t test. KOA: knee osteoarthritis; miRNA: microRNA [Color figure can be viewed at wileyonlinelibrary.com]

3.2 | hsa-miR-582-5p and hsa-miR-424-5p were significantly decreased in KOA sclerotic bone compared with nonsclerotic bone

It is well accepted that all parts of the joint, especially articular cartilage and SCB, contribute to KOA pathology. Clinically, patients with KOA often show cartilage degradation associated with SCB sclerosis. In this study, we identified the characteristics of sclerotic and nonsclerotic SCB in KOA. X-ray detection showed an obvious joint clearance narrowing and SCB sclerosis in the medial compartment (Figure 3a). A representative sample from total knee arthroplasty of KOA patient showed the sclerotic and nonsclerotic areas of knee tibia plate (Figure 3b). These two areas were subsequently dissected into small squares for morphological analysis. 3D reconstruction analysis of μCT scanning showed that the microstructure of sclerotic SCB was thicker and denser than the nonsclerotic SCB (Figure 3c). Alcian Blue Hematoxylin/Orange G (ABH/OG) staining of the sclerotic histological section also pointed out its changes with a thicker SCB and thinner damaged cartilage appearance than nonsclerotic section (Figure 3d). Morphometric analysis of μCT data indicated that the bone volume/total volume (BV/TV), bone mineral density (BMD) and trabecular bone thickness (Tb. Th) of sclerotic bone trabeculae were higher than nonsclerotic bone and the trabecular bone separation (Tb. Sp) and trabecular bone pattern factor (Tb. Pf) were conversely lower (Figure 3e–i). These findings revealed that bone remodeling in the sclerotic area was more active than non-sclerotic area, which probably due to the excessive osteogenic differentiation of stem cells.

Recent studies suggest that miRNAs can impede SCB sclerosis by downregulation of osteogenic differentiation. According to this, we conducted a second validation to determine if these differentially expressed miRNAs were involved in the pathology of SCB sclerosis. We then collected six sclerotic bones and four nonsclerotic bones from six KOA patients and detected the expression levels of the two candidate miRNAs. As we speculated, hsa-miR-582-5p and

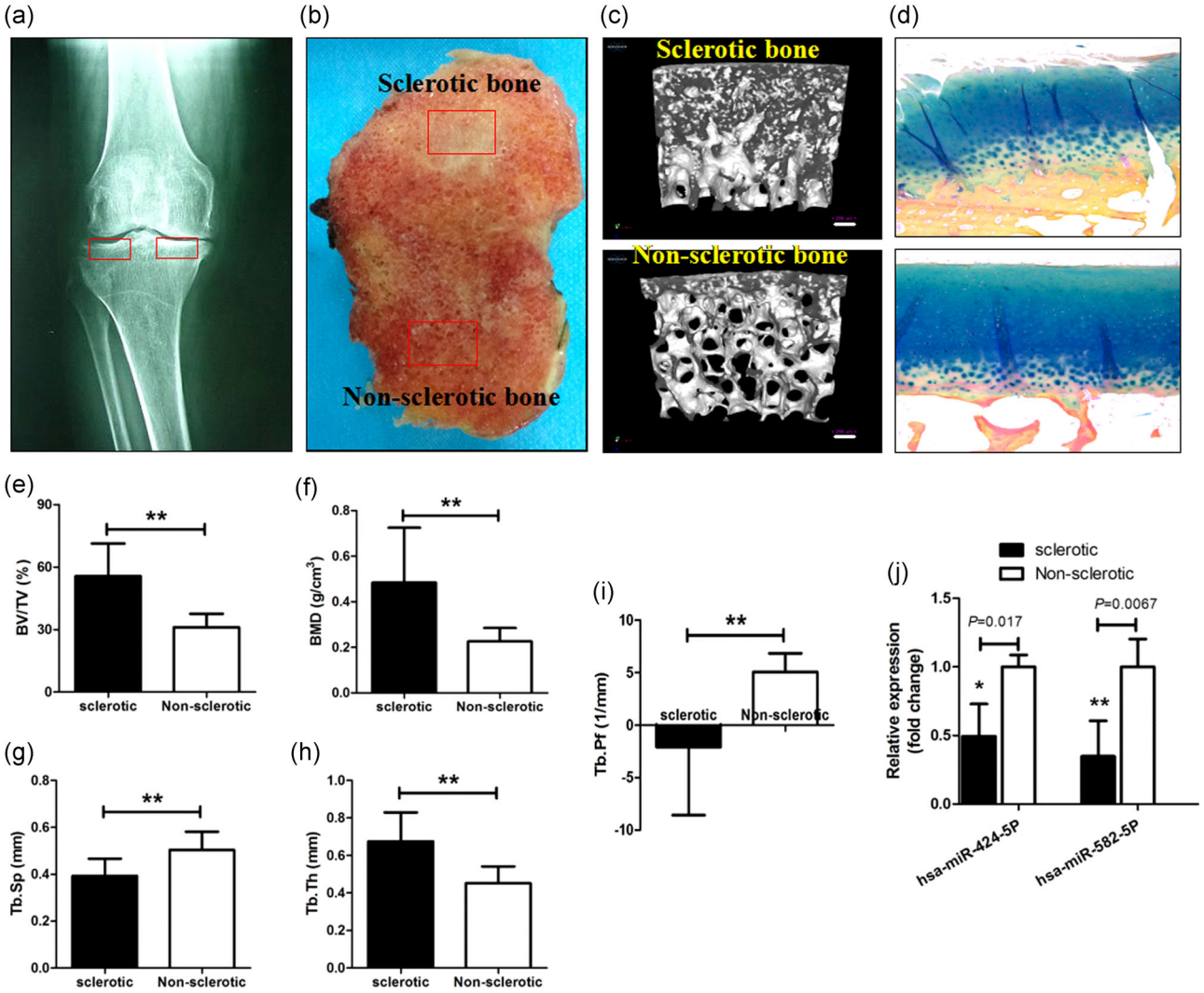

FIGURE 3 Expression of hsa-miR-582-5p and hsa-miR-424-5p in the subchondral bone of knee osteoarthritis (KOA) patients was confirmed to be lower in sclerosis area than nonsclerosis area. (a–c) X-ray, gross appearance and micro-computed tomography (μCT) 3D image were used to distinguish the sclerotic area and nonsclerotic area to facilitate the next subchondral bone (SCB) validation. (d) Alcian Blue Hematoxylin/Orange G staining showed the structure of cartilage and subchondral bone in KOA sclerotic area and nonsclerotic area. (e–i) The quantification of SCB trabecular bone parameters measured by μCT. (j) As blood sample validation, hsa-miR582-5p and hsa-miR424-5p have the same expression tendency between sclerotic bone and nonsclerotic bone. All data are shown as mean ± SD. $^{*}p < 0.05$, $^{**}p < 0.01$. *p* Values were determined by the Student *t* test. BV/TV: Bone Volume/Total Volume; BMD: Bone Mineral Density; Tb.Th: Trabecular bone Thickness; Tb.Sp: Trabecular bone Separation; Tb.Pf: Trabecular bone pattern factor [Color figure can be viewed at wileyonlinelibrary.com]

hsa-miR-424-5p were significantly downregulated in SCB sclerotic area compared with the nonsclerotic area (Figure 3j).

3.3 | Potential gene targets and pathways regulated by identified miRNAs

To identify the target genes of those differentially expressed miRNAs, we used three databases as follows: Targetscan, microRNA, and PITA. Finally, 225 target genes that appeared in all three databases (Figure 4a) were selected as the target genes of the candidate miRNAs. To determine the biological relevance of these potential target genes, we conducted an enrichment pathway analysis with GO and KEGG. Analysis with GO biological process indicated that these highly correlated target genes were involved in BMP (Bone Morphogenetic Protein) and transforming growth factor β (TGF β) receptor signaling pathway. KEGG pathway analysis indicated that these target genes were participated in signaling pathways regulating pluripotency of stem cells, TGF β, hippo, and AMPK (Adenosine 5'-Monophosphate-activated Protein Kinase) signaling pathway (Figure 4b,c), these signaling pathways are all involved in OA pathogenesis (Wang et al., 2017a; Wu et al., 2012; Ying et al., 2018).

3.4 | miR-582-5p downregulates osteogenic differentiation while upregulates adipogenic differentiation of MSCs

First, C3H10T1/2 mesenchymal progenitor cells were induced to osteoblast and adipocyte. We found that two differential expressed

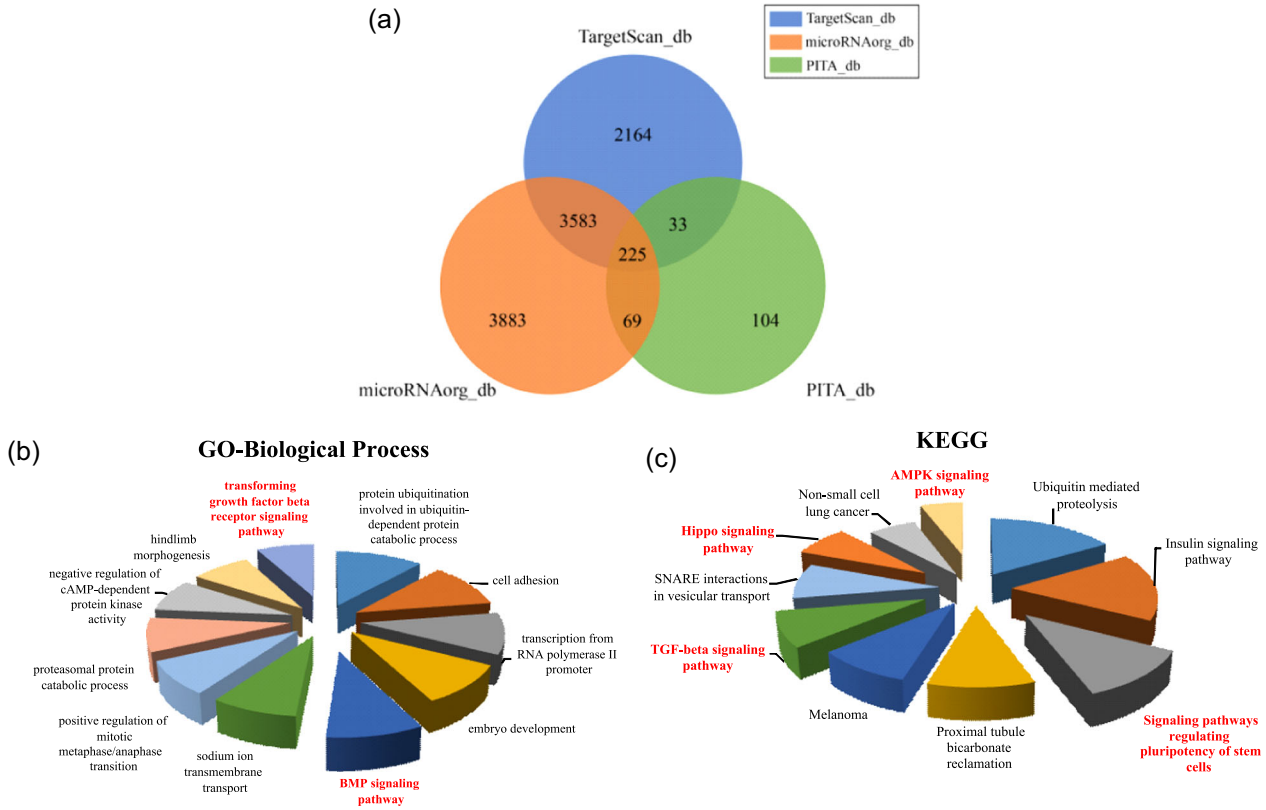

FIGURE 4 Blue pie represents TargetScan database which predicts 6,003 genes, microRNAorg database (orange pie) predicts 7,760 genes, meanwhile green pie (PITA database) predicts 431 genes, 225 genes showed in three predict databases were chosen as target genes for the next enrichment pathway analysis (a), GO biological process predicts two pathways (b) and KEGG predicts four pathways that highly related to OA which highlighted by red color (c). GO: Gene Ontology; KEGG: Kyoto Encyclopedia Genes and Genomes; OA: osteoarthritis; TGF β: transforming growth factor β [Color figure can be viewed at wileyonlinelibrary.com]

miRNAs identified in sclerotic SCB in this study were also detected in C3H10T1/2 cells during osteoblast and adipocyte differentiation. Surprisingly, mmu-mir-322-5p showed no difference compared with control (Figure 5a), while mmu-miR-582-5p was downregulated when MSCs were differentiated into osteoblasts and upregulated when MSCs were differentiated into adipocytes (Figure 5b), further suggesting miR-582-5p may contribute to the MSCs pluripotency.

To elucidate the exact roles of miR-582-5p in MSC differentiation, synthetic mimics and inhibitor of miR-582-5p were transfected into MSCs. The concentration of 37.5 nM mimics and 50 nM inhibitor were used for transfection about 16 hr, same concentration of mimics NC (negative control) and inhibitor NC were added to another two groups of cells as the negative control. After transfection, each group was induced to differentiate toward osteogenic or adipogenic lineage by culturing C3H10T1/2 cells with OIM or AIM, osteogenesis and adipogenesis markers were tested by ALP/Oil red O staining, qRT-PCR, and western blot analysis. The results showed that miR-582-5p could significantly impede osteogenic differentiation, demonstrated by decreased ALP activity (Figure 5c) and mRNA/protein levels of Runx2 and ALP (Figure 5d,f). In contrast, overexpression of miR-582-5p may promote MSC adipogenic differentiation with significantly increased Oil red O staining (Figure 5c) and the expression levels of PPARγ and C/EBPα (Figure 5d,g). Conversely, miR-582-5p inhibitor could efficiently reverse this differentiation potential. Compared with the negative control, miR-582-5p inhibitor could obviously accelerate osteogenic differentiation of MSCs by upregulating the activity of ALP (Figure 5c) and mRNA/protein levels of ALP and Runx2 (Figure 5d,f). Simultaneously, adipogenic differentiation of MSCs was obviously depressed by miRNA inhibitor as the reduction of Oil red O staining (Figure 5c) and mRNA/protein levels of PPARγ and C/EBPα (Figure 5d,g). The gain and loss of miR-582-5p function indicated that it could downregulates osteogenic differentiation while upregulates adipogenic differentiation of MSCs.

3.5 | Runx2 was directly targeted by miR-582-5p

The predicted potential targets of miR-582-5p in osteogenic and adipogenic differentiation include LRP6, RICTOR, Runx2 based on the online databases described above. To identify the direct targets of miR-582-5p, the reporter constructs of their 3′UTR were established and luciferase reporter assay was performed (Figure 6a). Only the luciferase activity of Runx2 3′UTR reporter was inhibited by miR-582-5p mimics (Figure 6b,d). To further determine if miR-582-5p directly binds to 3′UTR of Runx2, we constructed the mut-Runx2 3′UTR reporter transfected with

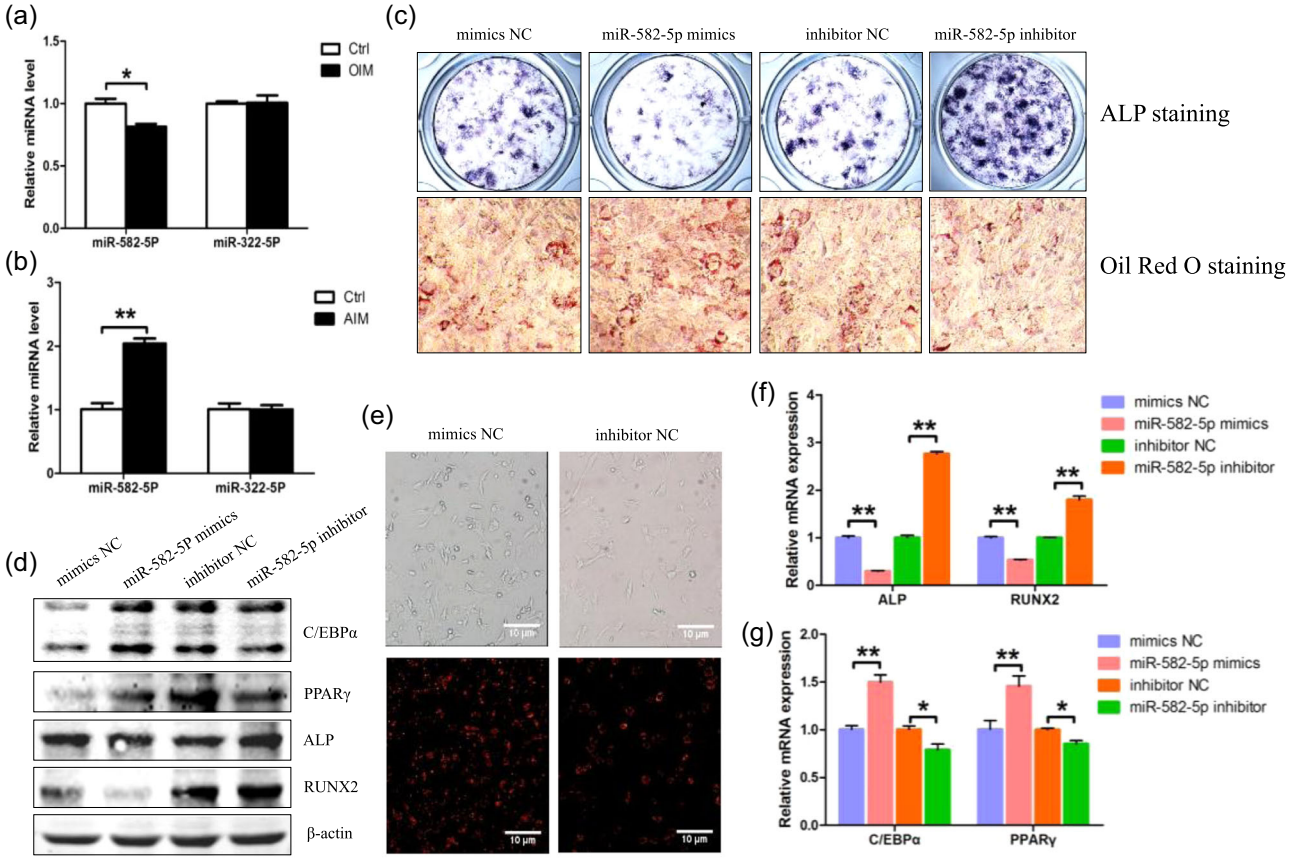

FIGURE 5 Expression of miR-582-5p was downregulated during osteogenic differentiation of MSCs and upregulated during adipogenic differentiation of MSCs and mmu-miR-322-5p levels were not changed when MSCs were cultured under OIM or AIM condition (a, b). The transfection efficiency of mimics NC and inhibitor NC in MSCs was approximately beyond 90% (e). Overexpression of miR-582-5p inhibited osteogenic differentiation while facilitated adipogenic differentiation of MSCs compared with negative control and inhibition of miR-582-5p showed the opposite effect (c). Overexpression of miR-582-5p could decrease the mRNA and protein levels of osteogenesis markers such as ALP and Runx2 which simultaneously increase the expression of adipogenic markers including C/EBPα and PPARγ. In contrast, inhibition of miR-582-5p could effectively reverse the aforementioned situation (d, f, g). All the staining data were confirmed in triplicate. All data are shown as mean ± SD. $^{*}p < 0.05$, $^{**}p < 0.01$. *p* Values were determined by the Student *t* test. AIM: adipocyte-inducing medium; xALP: alkaline phosphatase; mRNA: messenger RNA; MSC: mesenchymal stem cell; NC: negative control; OIM: osteoblast-induced medium; PPAR: peroxisome proliferator-activated receptor [Color figure can be viewed at wileyonlinelibrary.com]

miR-582-5p mimics. The results showed that mutation of 3′UTR abolished the inhibitory effect of miR-582-5p on Runx2 (Figure 6e). Consistent with the results of reporter assays, transient transfection of miR-582-5p mimics in C3H10T1/2 cells reduced the mRNA and protein level of Runx2. In contrast, suppression of the endogenous miR-582-5p using the synthetic inhibitor increased Runx2 mRNA and protein level (Figure 5e,f).

4 | DISCUSSION

KOA is a whole joint disease affecting not only cartilage, bone, and synovium, but also bone marrow, muscle, menisci, ligament and neural tissue (Brandt, Radin, Dieppe, & van de Putte, 2006). To date, it's difficult to determine that KOA is initiated from which part of joint tissue. Articular cartilage is an avascular tissue, while the underlying bone plate is highly vascularized and provide more than 50% of the hyaline cartilage nutrition (Imhof et al., 2000). Many studies suggested that SCB remodeling was taken place in the onset of KOA (Maerz et al., 2016; Poulet et al., 2015; Zhao et al., 2016). At the early stage of KOA, bone marrow lesion (BML) appears as increased remodeling of SCB and marrow in the response of mechanical overload, it is closely related to cartilage loss and development of KOA (Hunter et al., 2006; Roemer et al., 2009). With the development of the disease, uncoupled SCB remodeling leads to bone sclerosis which may interfere with the articular cartilage hemostasis. Previous studies showed that inhibition of SCB sclerosis could prevent cartilage degeneration (Lin et al., 2018; Zhen et al., 2013). A series of molecules were involved in the complicated process of SCB sclerosis, the underlying mechanisms have not been elucidated. However, miRNAs have been reported to have an important role in the regulation of the catabolism and anabolism of bone and cartilage. In our study, differentially expressed miRNAs were identified through microarray analysis. After validation with

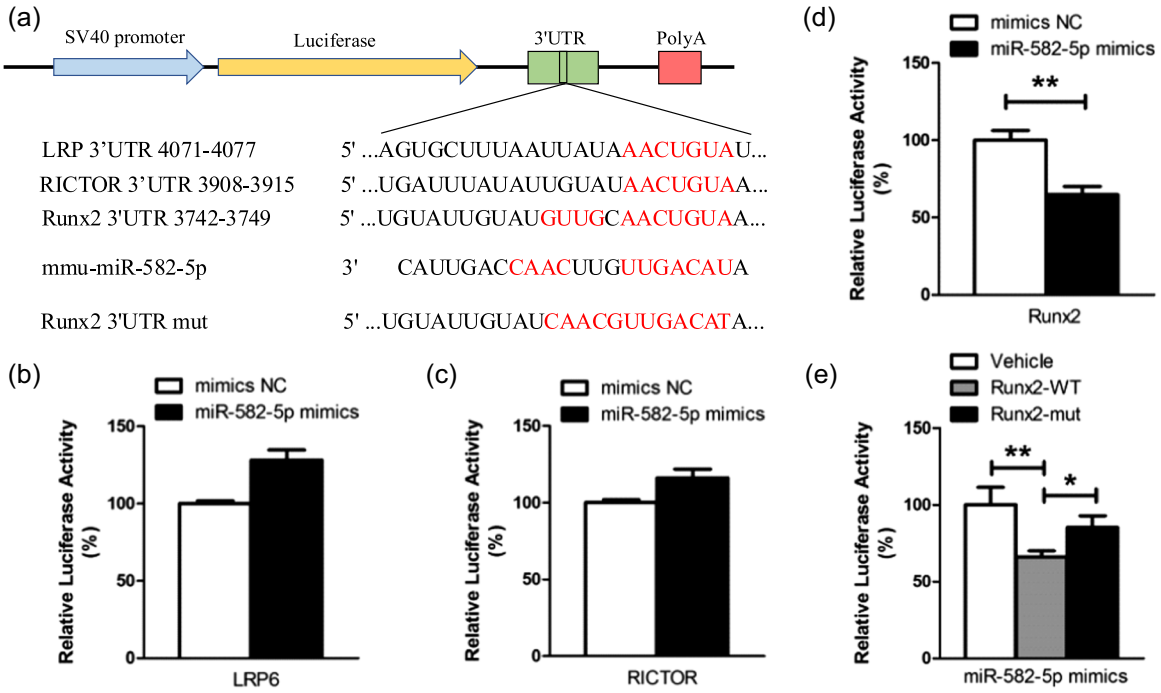

FIGURE 6 miR-582-5P directly targeted Runx2. A schematic diagram illustrated the 3′UTR fragments of LRP, RICTOR, Runx2 (a). Transfection of miR-582-5p in 293T cells decreased the luciferase activity of Runx2 (d), while had no effects on LRP and RICTOR constructs (b, c). The miR-582-5p lost its inhibitory effect on the 3′UTR construct of Runx2 when its putative miR-582-5p binding site was mutated (e). All data are shown as mean ± SD. $^{*}p < 0.05$, $^{**}p < 0.01$. *p* Values were determined by the Student *t* test. LRP: low-density lipoprotein receptor-related protein; NC: negative control; RICTOR: rapamycin-insensitive companion of mammalian target of rapamycin; UTR: untranslated region [Color figure can be viewed at wileyonlinelibrary.com]

whole blood samples, two differentially expressed miRNAs have been identified in KOA patients. To examine our hypothesis, we then conduct a tissue-specific validation by qRT-PCR. Results showed the expression of hsa-miR-424-5p and hsa-miR-582-5p were decreased in KOA sclerotic SCB compared with nonsclerotic bone. We believed that these two miRNAs may involve in the pathogenesis of SCB sclerosis.

miRNAs play regulatory roles in target genes expression to participate in various biological functions. Potential target genes and pathway analysis show that these two miRNAs may involve in TGF-β, BMP, AMPK, Hippo signaling pathways and stem cells pluripotency and differentiation. To date, these pathways have been demonstrated to be essential for the homeostasis of cartilage and SCB. For instance, increasing evidence suggested that inhibition TGF-β and BMP signaling pathway could attenuate cartilage degradation and SCB sclerosis (Chen et al., 2015; Hellingman et al., 2011; Wang et al., 2017a; Zhen et al., 2013). Hippo signaling pathway activation could downregulate the expression of Runx2 and Col10 to prevent chondrocyte hypertrophy. Moreover, the majority of these signaling pathways are involved in the regulation of pluripotency and differentiation of stem cells (Cao, Lv, & Lv, 2015; Cheung et al., 2014; Wang, Cai, Cai, & Chen, 2013), which may break the balance between osteogenesis and adipogenesis of MSCs subsequently leading to SCB sclerosis and OA development.

MSCs could be easily collected and exhibit the strong ability of self-renew and multi-directional differentiation potential (Trounson & McDonald, 2015), such as differentiation into chondrocytes, osteoblasts and other types of cells under different microenvironment. Studies showed that MSCs were recruited to SCB and differentiated into osteoblasts for bone formation during or after anterior cruciate ligament transection (ACLT; Zhen et al., 2013). In clinics, MSC cells derived from OA patients showed high osteogenic differentiation capacity and low adipogenic differentiation tendency (Lian et al., 2017; Salamon et al., 2013; Xia et al., 2016), uncoupled with osteoclast bone resorption leading to subsequent SCB sclerosis. Reversing this differentiation tendency of MSCs may inhibit this pathological process. miRNAs have been demonstrated to be able to induce MSCs differentiation. For example, inhibition of miR-146b facilitates human bone MSCs differentiate to chondrocytes (Budd, de Andrés, & Sanchez-Elsner, 2017) and miR-27a could upregulate osteogenic differentiation of MSCs (You, Pan, Chen, Gu, & Chen, 2016). MiR-31-5p and miR-424-5p were decreased in OA cartilage derived MSCs, as these cells show lower adipogenic and higher osteogenic capacity (Xia et al., 2016). In our study, miR-582-5p was reduced during osteogenic differentiated MSCs, simultaneously elevated in adipogenic differentiated MSCs. Inconsistent with previous studies, miR-424-5p expression was not changed during MSC differentiation. This discrepancy may ascribe to the different sources of MSCs used in two studies. The cells used in the first study were derived from human articular cartilage and the cells used in in vitro studies were from those of mouse origin.

miR-582-5p has already been studied in several previous studies. Its' overexpression could targeting FOXC1 to repressing the activity of salivary adenoid cystic carcinoma cell (Wang et al., 2017b), facilities colorectal cancer cell and prostate cancer cell proliferation (Shu, Chen, & Ding, 2016; Zhanget al., 2015). Moreover, it can also impede apoptosis of monocytes involving in the progression of tuberculosis (Liu, Jiang, Wang, Zhai, & Cheng, 2013). To date, the role of miR-582-5p in the regulation of stem cell pluripotency and KOA development has not been reported. We discovered that miR-582-5p was significantly downregulated in SCB of KOA patients and altered during osteogenesis and adipogenesis of C3H10T/2 cells. ALP and Oil red O staining indicated miR-582-5p as a negative regulator of osteoblast differentiation and a positive regulator of adipocyte differentiation. qRT-PCR and western blot analysis showed that transfecting of mmu-miR-582-5p mimics could downregulate Runx2 and ALP expression and increase C/EBPα and PPAR-γ expression. Inhibition of endogenous miR-582-5p was inversely increased Runx2 and ALP mRNA and protein levels, simultaneously decrease C/EBPα and PPAR-γ levels in vitro. Luciferase reporter assay showed that Runx2 was a directly target of miR-582-5p. Therefore, we hypothesized that miR-582-5p might regulate osteogenesis and adipogenesis through Runx2 in MSCs, participating in the pathological process of KOA. MSCs derived from KOA patients showed high osteogenic activity and low adipogenic activity and overexpression of miR-582-5p could partially reverse the differentiation potential of MSCs.

Even though SCB sclerosis is quite important in KOA progression, majority of KOA-related miRNAs were found to participate in cartilage degradation, chondrocytes apoptosis, inflammation, et al. In other words, SCB specific miRNAs remain elusive. Analyses of this study presented the first indication that miR-582-5p, a stem cell-specific miRNA, acted as an inhibitor of stem cell osteogenesis and an agonist for adipogenesis by targeting Runx2. The main result of this study indicates that miR-582-5p might be a potential target to prevent SCB sclerosis and to treat KOA.

ACKNOWLEDGMENTS

This study was supported by the National Natural Science Foundation of China (Grant No. 81774332, 81774346, 81873324, and 81873325). This study has been partially supported by Zhejiang grants funded by Provincial Natural Science Foundation of China (Grant No. LY16H270010, LY18H270004), the State Administration of Traditional Chinese Medicine of Zhejiang Province (Grant No. 2018ZZ011, 2018ZA034, and 2019ZQ018), the Medical Health Science and Technology Project of Health Commission of Zhejiang Province (Grant No. 2019RC225), the Opening Project of Zhejiang Provincial Preponderant and Characteristic Subject of Key University (Chinese Traditional Medicine) of Zhejiang Chinese Medical University (Grant No. ZYX2018001 and ZYX2018004), the Project of Zhejiang Chinese Medical University (Grant No. 2C01801-01).

AUTHOR CONTRIBUTIONS

All authors were involved in drafting the article and critically revising important intellectual content. Conception: H. J., P. T., J. L., and L. X. Study design: H. J., J. L., P. T., P. W., and D. C. Data acquisition: P. W., R. D., B. W., Z. L., J. Y., C. X., S. H., W. W., Q. S., P. Z., and Q. G. Data analysis: P. W., R. D., H. J., and B. W. Data interpretation: P. W., R. D., P. T., J. L., and H. J. All authors approved the final version to be published.

DATA ACCESSIBILITY

The data that support the findings of this study are available from the corresponding author upon reasonable request.

ETHICS STATEMENT

Ex vivo studies with human blood and knee joint tissues were approved by the Ethics Committee of The First Affiliated Hospital of Zhejiang Chinese Medical University (2018-ZX-026-01).

ORCID

Pinger Wang http://orcid.org/0000-0002-4124-0188
Chenjie Xia http://orcid.org/0000-0002-5987-4146

REFERENCES

Alcaraz, M. J., Megías, J., García-Arnandis, I., Clérigues, V., & Guillén, M. I. (2010). New molecular targets for the treatment of osteoarthritis. *Biochemical Pharmacology*, *80*(1), 13–21.

Brandt, K. D., Radin, E. L., Dieppe, P. A., & van de Putte, L. (2006). Yet more evidence that osteoarthritis is not a cartilage disease. *Annals of the Rheumatic Diseases*, *65*(10), 1261–1264.

Budd, E., de Andrés, M. C., Sanchez-Elsner, T., & R. O. C. O. (2017). MiR-146b is down-regulated during the chondrogenic differentiation of human bone marrow derived skeletal stem cells and up-regulated in osteoarthritis. *Scientific Reports*, *7*, 46704.

Cao, Y., Lv, Q., & Lv, C. (2015). MicroRNA-153 suppresses the osteogenic differentiation of human mesenchymal stem cells by targeting bone morphogenetic protein receptor type II. *International Journal of Molecular Medicine*, *36*(3), 760–766.

Chen, H., & Tian, Y. (2017). MiR-15a-5p regulates viability and matrix degradation of human osteoarthritis chondrocytes via targeting VEGFA. *Bioscience Trends*, *10*(6), 482–488.

Chen, R., Mian, M., Fu, M., Zhao, J. Y., Yang, L., Li, Y., & Xu, L. (2015). Attenuation of the progression of articular cartilage degeneration by inhibition of TGF-beta1 signaling in a mouse model of osteoarthritis. *American Journal of Pathology*, *185*(11), 2875–85.

Cheung, K. S., Sposito, N., Stumpf, P. S., Wilson, D. I., Sanchez-Elsner, T., & Oreffo, R. O. (2014). MicroRNA-146a regulates human foetal femur derived skeletal stem cell differentiation by down-regulating SMAD2 and SMAD3. *PLOS One*, *9*(6), e98063.

Glyn-Jones, S., Palmer, A. J. R., Agricola, R., Price, A. J., Vincent, T. L., Weinans, H., & Carr, A. J. (2015). Osteoarthritis. *Lancet*, *386*, 376–387.

Hellingman, C. A., Davidson, E. N. B., Koevoet, W., Vitters, E. L., van den Berg, W. B., van Osch, G. J. V. M., & van der Kraan, P. M. (2011). Smad signaling determines chondrogenic differentiation of bone-marrow-derived mesenchymal stem cells: Inhibition of Smad1/5/8P prevents terminal differentiation and calcification. *Tissue Engineering. Part A*, *17*(7–8), 1157–67.

Hunter, D. J., Zhang, Y., Niu, J., Goggins, J., Amin, S., LaValley, M. P., … Felson, D. T. (2006). Increase in bone marrow lesions associated with cartilage loss: A longitudinal magnetic resonance imaging study of knee osteoarthritis. *Arthtitis and Rheumatism*, *54*(5), 1529–35.

Imhof, H., Sulzbacher, I., Grampp, S., Czerny, C., Youssefzadeh, S., & Kainberger, F. (2000). Subchondral bone and cartilage disease: A rediscovered functional unit. *Investigative Radiology*, *35*(10), 581–588.

Juneja, S. C., Ventura, M., Jay, G. D., & Veillette, C. (2016). A less invasive approach of medial meniscectomy in rat : A model to target early or less severe human osteoarthritis. *Journal of Arthritis.*, *5*(2), 193.

Kao, H. W., Pan, C. Y., Lai, C. H., Wu, C. W., Fang, W. L., Huang, K. H., & Lin, W. C. (2017). Urine miR-21-5p as a potential non-invasive biomarker for gastric cancer. *Oncotarget*, *8*(34), 56389–56397.

Kung, L. H. W., Zaki, S., Ravi, V., Rowley, L., Smith, M. M., Bell, K. M., … Little, C. B. (2017). Utility of circulating serum miRNAs as biomarkers of early cartilage degeneration in animal models of post-traumatic osteoarthritis and inflammatory arthritis. *Osteoarthritis and Cartilage*, *25*(3), 426–434.

Lawrence, R. C., Felson, D. T., Helmick, C. G., Arnold, L. M., Choi, H., Deyo, R. A., … Wolfe, F. (2008). Estimates of the prevalence of arthritis and other rheumatic conditions in the United States. Part II. *Arthtitis and Rheumatism*, *58*(1), 26–35.

Lewis, B. P., Burge, C. B., & Bartel, D. P. (2005). Conserved seed pairing, often flanked by adenosines, indicates that thousands of human genes are microRNA targets. *Cell*, *120*(1), 15–20.

Lian, W. S., Wu, R. W., Lee, M. S., Chen, Y. S., Sun, Y. C., Wu, S. L., … Wang, F. S. (2017). Subchondral mesenchymal stem cells from osteoarthritic knees display high osteogenic differentiation capacity through microRNA-29a regulation of HDAC4. *Journal of Molecular Medicine*, *95*(12), 1327–1340.

Lin, C., Shao, Y., Zeng, C., Zhao, C., Fang, H., Wang, L., … Xian, C. J. (2018). Blocking PI3K/AKT signaling inhibits bone sclerosis in subchondral bone and attenuates post-traumatic osteoarthritis. *Journal of Cellular Physiology*, *233*, 6135–6147.

Liu, Y., Jiang, J., Wang, X., Zhai, F., & Cheng, X. (2013). miR-582-5p is upregulated in patients with active tuberculosis and inhibits apoptosis of monocytes by targeting FOXO1. *PLOS One*, *8*(10), e78381.

Livak, K. J., & Schmittgen, T. D. (2001). Analysis of relative gene expression data using real-time quantitative PCR and the 2(-Delta Delta C(T)) Method. *Methods*, *25*(4), 402–408.

Lories, R. J., & Luyten, F. P. (2011). The bone-cartilage unit in osteoarthritis. *Nature Reviews Rheumatology*, *7*(1), 43–49.

Madry, H., van Dijk, C. N., & Mueller-Gerbl, M. (2010). The basic science of the subchondral bone. *Knee Surgery, Sports Traumatology, Arthroscopy*, *18*(4), 419–33.

Maerz, T., Kurdziel, M., Newton, M. D., Altman, P., Anderson, K., Matthew, H. W. T., & Baker, K. C. (2016). Subchondral and epiphyseal bone remodeling following surgical transection and noninvasive rupture of the anterior cruciate ligament as models of post-traumatic osteoarthritis. *Osteoarthritis and Cartilage*, *24*(4), 698–708.

Petrozza, V., Pastore, A. L., Palleschi, G., Tito, C., Porta, N., Ricci, S., … Fazi, F. (2017). Secreted miR-210-3p as non-invasive biomarker in clear cell renal cell carcinoma. *Oncotarget*, *8*(41), 69551–69558.

Poulet, B., de Souza, R., Kent, A. V., Saxon, L., Barker, O., Wilson, A., … Pitsillides, A. A. (2015). Intermittent applied mechanical loading induces subchondral bone thickening that may be intensified locally by contiguous articular cartilage lesions. *Osteoarthritis and Cartilage*, *23*(6), 940–948.

Prasadam, I., Batra, J., Perry, S., Gu, W., Crawford, R., & Xiao, Y. (2016). Systematic identification, characterization and target gene analysis of microRNAs involved in osteoarthritis subchondral bone pathogenesis. *Calcified Tissue International*, *99*(1), 43–55.

Roemer, F. W., Guermazi, A., Javaid, M. K., Lynch, J. A., Niu, J., Zhang, Y., … Nevitt, M. C. (2009). Change in MRI-detected subchondral bone marrow lesions is associated with cartilage loss: The MOST Study. A longitudinal multicentre study of knee osteoarthritis. *Annals of the Rheumatic Diseases*, *68*(9), 1461–1465.

Salamon, A., Jonitz-Heincke, A., Adam, S., Rychly, J., Müller-Hilke, B., Bader, R., … Peters, K. (2013). Articular cartilage-derived cells hold a strong osteogenic differentiation potential in comparison to mesenchymal stem cells in vitro. *Experimental Cell Research*, *319*(18), 2856–65.

Shu, Z., Chen, L., & Ding, D. (2016). miR-582-5P induces colorectal cancer cell proliferation by targeting adenomatous polyposis coli. *World Journal of Surgical Oncology*, *14*(1), 239.

Tang, X., Wang, S., Zhan, S., Niu, J., Tao, K., Zhang, Y., & Lin, J. (2016). The prevalence of symptomatic knee osteoarthritis in china: Results from the china health and retirement longitudinal study. *Arthritis Rheumatology*, *68*(3), 648–53.

Trounson, A., & McDonald, C. (2015). Stem cell therapies in clinical trials: Progress and challenges. *Cell Stem Cell*, *17*(1), 11–22.

Vilahur, G. (2017). Relevance of low miR-30c-5p levels in atherogenesis: A promising predictive biomarker and potential therapeutic target. *Cardiovascular Research*, *113*(13), 1536–1537.

Wang, Q., Cai, J., Cai, X. H., & Chen, L. (2013). miR-346 regulates osteogenic differentiation of human bone marrow-derived mesenchymal stem cells by targeting the Wnt/beta-catenin pathway. *PLOS One*, *8*(9), e72266.

Wang, W. W., Chen, B., Lei, C. B., Liu, G. X., Wang, Y. G., Yi, C., … Zhang, S. Y. (2017a). miR-582-5p inhibits invasion and migration of salivary adenoid cystic carcinoma cells by targeting FOXC1. *Japanese Journal of Clinical Oncology*, *47*(8), 690–698.

Wang, Y. J., Shen, M., Wang, S., Wen, X., Han, X. R., Zhang, Z. F., … Zheng, Y. L. (2017b). Inhibition of the TGF-β1/Smad signaling pathway protects against cartilage injury and osteoarthritis in a rat model. *Life Sciences*, *189*, 106–113.

Wu, L., Huang, X., Li, L., Huang, H., Xu, R., & Luyten, W. (2012). Insights on biology and pathology of HIF-1alpha/-2alpha, TGFbeta/BMP, Wnt/beta-catenin, and NF-kappaB pathways in osteoarthritis. *Current Pharmaceutical Design*, *18*(22), 3293–312.

Xia, Z., Ma, P., Wu, N., Su, X., Chen, J., Jiang, C., … Wu, Z. (2016). Altered function in cartilage derived mesenchymal stem cell leads to OA-related cartilage erosion. *American Journal of Translational Research*, *8*(2), 433–446.

Ying, J., Wang, P., Zhang, S., Xu, T., Zhang, L., Dong, R., … Jin, H. (2018). Transforming growth factor-beta1 promotes articular cartilage repair through canonical Smad and Hippo pathways in bone mesenchymal stem cells. *Life Sciences*, *192*, 84–90.

You, L., Pan, L., Chen, L., Gu, W., & Chen, J. (2016). MiR-27a is Essential for the Shift from Osteogenic Differentiation to Adipogenic Differentiation of Mesenchymal Stem Cells in Postmenopausal Osteoporosis. *Cellular Physiology and Biochemistry*, *39*(1), 253–65.

Yu, C., & Wang, Y. (2018). MicroRNA-19a promotes cell viability and migration of chondrocytes via up-regulating SOX9 through NF-κB pathway. *Biomedicine and Pharmacotherapy*, *98*, 746–753.

Zhang, Y., Huang, W., Ran, Y., Xiong, Y., Zhong, Z., Fan, X., … Ye, Q. (2015). miR-582-5p inhibits proliferation of hepatocellular carcinoma by targeting CDK1 and AKT3. *Tumour Biology*, *36*(11), 8309–16.

Zhao, W., Wang, T., Luo, Q., Chen, Y., Leung, V. Y. L., Wen, C., … Lu, W. W. (2016). Cartilage degeneration and excessive subchondral bone formation in spontaneous osteoarthritis involves altered TGF-β signaling. *Journal of Orthopaedic Research*, *34*(5), 763–70.

Zhen, G., Wen, C., Jia, X., Li , Y., Crane, J. L., Mears, S. C., … Cao, X (2013). Inhibition of TGF-β signaling in mesenchymal stem cells of subchondral bone attenuates osteoarthritis. *Nature Medicine*, *19*(6), 704–714.

How to cite this article: Wang P, Dong R, Wang B, et al. Genome-wide microRNA screening reveals miR-582-5p as a mesenchymal stem cell-specific microRNA in subchondral bone of the human knee joint. *J Cell Physiol*. 2019;234: 21877–21888. https://doi.org/10.1002/jcp.28751